**Biophysical Journal, Volume *119***

## Supplemental Information

# Substrate Resistance to Traction Forces Controls Fibroblast Polarization

**Dimitris Missirlis, Tamás Haraszti, Lara Heckmann, and Joachim P. Spatz**

**Supplementary Table S1.** Reagents used in our study

| Reagent | Abbreviation | Supplier | Cat. No. |
|---|---|---|---|
| **Blebbistatin** | - | Sigma-Aldrich | B0560 |
| **Ethanol (pure)** | - | Roth | 9065.3 |
| **Bovine Serum Albumin** | BSA | Sigma-Aldrich | A4161 |
| **Bovine Plasma Fibronectin** | FN | Sigma-Aldrich | F1141 |
| **4% Paraformaldehyde in PBS** | PFA | Santa Cruz | sc-281962 |
| **Phalloidin-tetramethylrhodamine B isothiocyanate** | TRITC-Phalloidin | Sigma-Aldrich | P1951 |
| **4',6-Diamidino-2-Phenylindole, Dihydrochloride** | DAPI | Thermo-Fisher | D1306 |
| **Fluospheres™ Carboxylate-Modified Microspheres, 0.2 µm, red fluorescent** | - | Thermo-Fisher | F8810 |
| **Triethylamine** | - | Sigma-Aldrich | 471283 |
| **(3-Aminopropyl)triethoxysilane** | APTES | Sigma-Aldrich | A3648 |
| **Triton X-100** | - | Sigma-Aldrich | - |
| ***N*-(3-Dimethylaminopropyl)-*N′*-ethylcarbodiimide hydrochloride** | EDC | Sigma-Aldrich | 03450 |
| **Dimethyl sulfoxide** | DMSO | Sigma-Aldrich | D8418 |

**Supplementary Table S2.** Antibodies used in our study

| Antibody | Clone | Application / Dilution | Supplier | Cat. No. |
|---|---|---|---|---|
| **anti-paxillin** | 165/Paxillin | Immunofluorescence / 1:100 | BD | 610619 |
| **anti-α-tubulin** | B-5-1-2 | Immunofluorescence / 1:1000 | Sigma | T6074 |
| **anti-pY** | PY99 | Immunofluorescence / 1:100 | Santa Cruz Biotechnology | sc-7020 |
| **anti-cellular fibronectin (EDA)** | DH1 | Immunofluorescence / 1:100 | Merck-Millipore | MAB1940 |
| **anti-fibronectin** | P1H11 | ELISA / 1:10000 | Merck-Millipore | MAB1926 |
| **anti-fibronectin** | A32 | ELISA / 1:5000 | Thermo-Fisher | CSI 005-32-02 |
| **anti-mouse HRP conjugate** | polyclonal | ELISA / 1:2000 | Santa Cruz Biotechnology | sc-2005 |
| **anti-mouse IgG AlexaFluor488 conjugate** | polyclonal | Immunofluorescence / 1:150 | Thermo-Fisher | A11001 |
| **anti-mouse IgG AlexaFluor647 conjugate** | polyclonal | Immunofluorescence / 1:150 Flow Cytometry | Thermo-Fisher | A31571 |
| **anti-rabbit IgG AlexaFluor647 conjugate** | polyclonal | Immunofluorescence / 1:150 | Thermo-Fisher | A21244 |
| **anti-rabbit IgG AlexaFluor568 conjugate** | polyclonal | Immunofluorescence / 1:150 | Thermo-Fisher | A11011 |

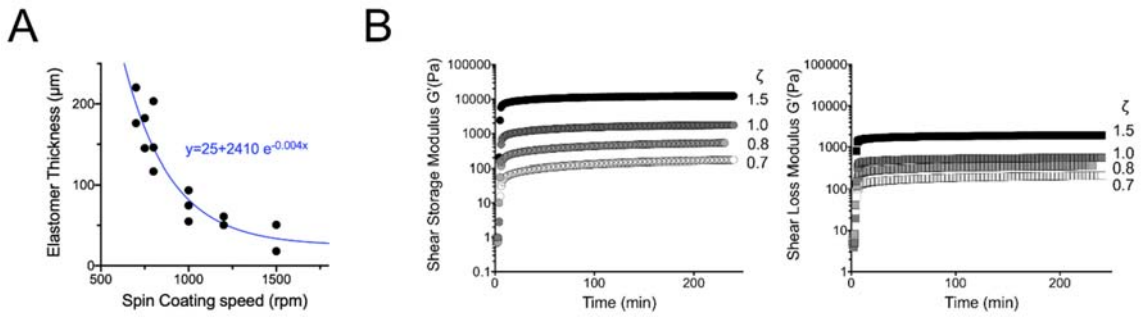


**Figure S1. A)** Effect of spin coating speed on elastomer thickness. 150-200 µl of 1:1 mixture of elastomer components from formulation CY52-276 (ζ=1.0) were spin coated on top of a circular glass coverslip (diameter of 15 mm), previously coated with fluorescent nanoparticles. Elastomers were then cross-linked for 3 hours at 65°C. The thickness of the elastomer was determined using confocal microscopy after coating the elastomer surface with a second layer of fluorescent nanoparticles and measuring the distance between the two fluorescent layers. **B)** The two components of the silicone elastomer (CY52-276) were thoroughly mixed, degassed and placed between two parallel plates of a rheometer within 15 minutes from mixing. The temperature was raised rapidly at 65°C and oscillatory measurements were initiated (t=0). The shear (G') and loss (G'') moduli were monitored over time using a frequency of 1 Hz and a strain of 5%. Both moduli showed a rapid increase within the first 5 minutes and reached a plateau within 200 minutes.

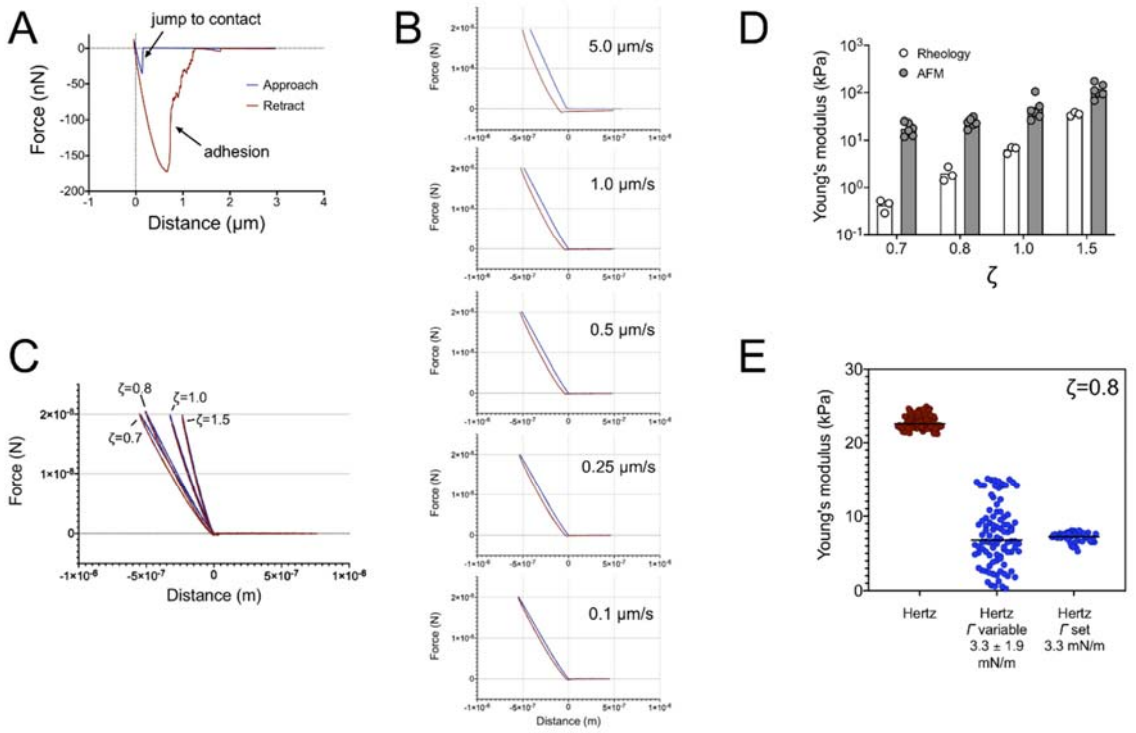


**Figure S2. A)** Force distance (F-d) curves obtained from AFM indentation measurements of an uncoated silicone elastomer (ζ=1.0) in ethanol. Both the approach (blue) and retraction (red) curves are presented. Tip adhesion to the substrate was very strong. **B)** F-d curves (blue: approach; red: retraction) derived from AFM indentation measurements of BSA-coated, soft silicone elastomers (ζ=0.7) at different indentation speeds revealed significant hysteresis. **C)** F-d curves (blue: approach; red: retraction) derived from AFM indentation measurements of BSA-coated elastomers of different ζ values at an indentation speed of 0.1 µm/s. **D)** Comparison of Young's modulus values of silicone elastomers derived from oscillatory rheology and AFM indentation measurements. A setpoint of 10 nN and an indentation speed of 1 µm/s were used for the AFM measurements and the Young's modulus was calculated using the standard Hertz model. For Young's moduli calculated from oscillatory rheology measurements a Poisson ratio of 0.495 was used and the shear modulus calculated at 1 Hz. **E)** Young's modulus values calculated for a silicone elastomer (ζ=0.8) after fitting F-d curves with the standard Hertz model, a modified Hertz model that has a variable solid surface tension term and after fixing the value of the solid surface term to corresponding to the best fit of the data.

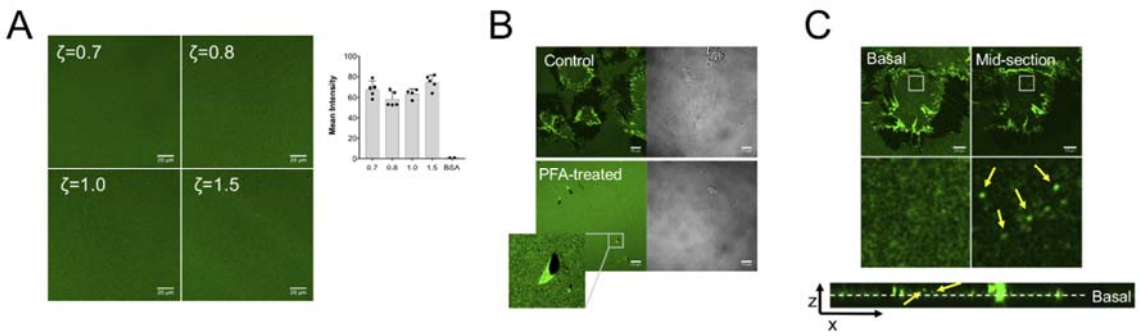


**Figure S3. A)** Confocal microscopy images of the surface of silicone elastomers coated with pre-labeled fluorescent fibronectin (FFN). Fluorescence was homogeneous over the substrate and fluorescent intensity was independent of elastomer mechanical properties. Quantification from 1 out of 2 independent experiments; each data point corresponds to the mean intensity at a different region of the elastomer, the column represents the mean and error bars the SD. **B)** Live-cell, confocal microscopy images of FFN-coated glass substrates, untreated (control) or treated with 4% PFA, 2 hours after seeding pHDF in supplemented medium. FFN remodeling by fibroblasts was inhibited by PFA treatment **C)** Live-cell, confocal microscopy images of FFN-coated glass substrates, 2 hours after pHDF seeding. Besides FFN fibril assembly, bright vesicles in the cell interior were observed, suggesting that cells internalized FFN. Scale bars: 10 μm.

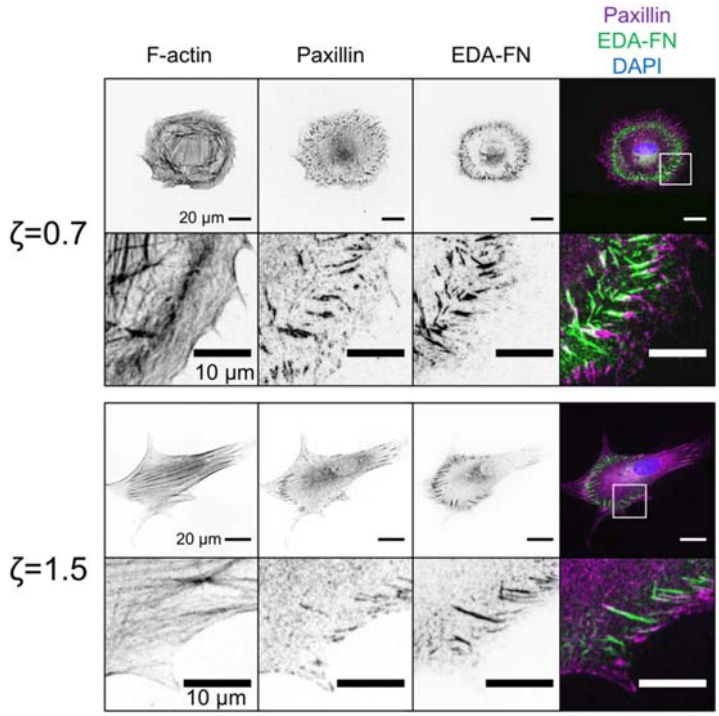


**Figure S4.** Confocal microscopy images of pHDF seeded for 4 hours on FN-coated silicone elastomers with indicated ζ ratios and immunostained against F-actin, paxillin and cell-secreted FN, which contains the EDA domain. Despite the lack of the adsorbed (coated) FN, fibroblasts assembled FN fibrils, which contained EDA-FN.

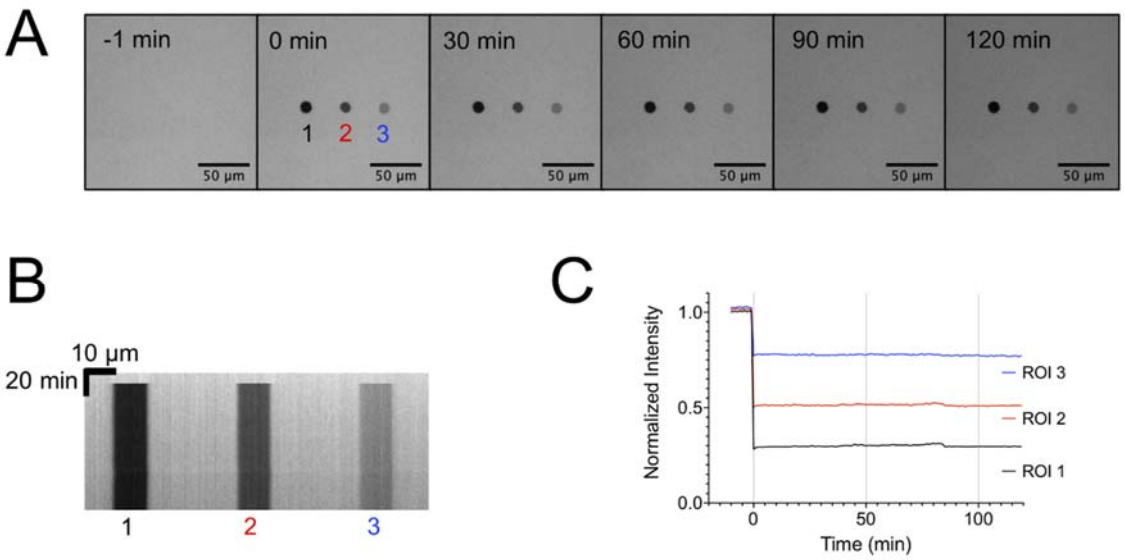


**Figure S5. A)** Epifluorescence microscopy images of silicone elastomers coated with pre-labeled fluorescent fibronectin (FFN) during a FRAP experiment. Three region of interest (ROI) were photo-bleached with different laser intensities. Selected images before and after the bleaching step are presented. **B)** Kymograph showing the absence of visible fluorescence recovery on the bleached ROIs. **C)** Quantification of fluorescence intensity over time for the bleached ROIs. Fluorescence intensity was corrected for overall bleaching and normalized to the background.

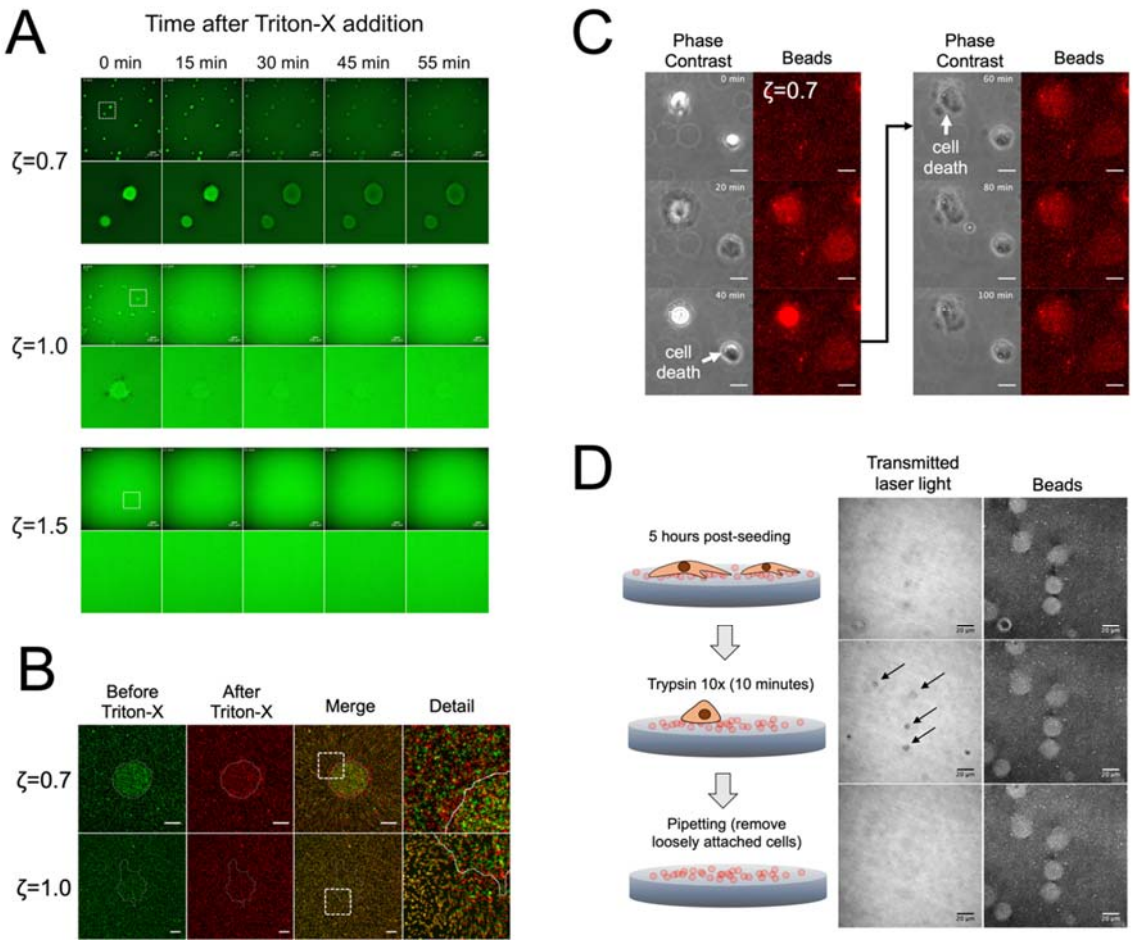


**Figure S6. A)** Still frames from live-cell, time-lapse epifluorescence microscopy imaging of silicone elastomers coated with pre-labeled fluorescent fibronectin (FFN). pHDF were cultured for 3 hours on top of the elastomers, before a concentrated solution of Triton-X was added to induce cell death and elimination of traction forces (t=0 min). FFN did not recover its initial homogeneous distribution prior to cell seeding on the softer elastomers. Scale bars: 100 μm. **B)** Confocal microscopy images (maximum projections for ζ=0.7) of fluorescent beads immobilized on elastomers coated with FN, before and after addition of Triton-X. pHDF were cultured for 3 hours (Before) prior to Triton-X addition. Images acquired 30-45 after Triton-X addition (After) revealed that beads did not return to a homogeneous distribution, indicative of their initial positions, upon elimination of cell tractions, indicating plastic deformations. Scale bars: 20 μm. **C)** Still frames from live-cell, time-lapse microscopy imaging of pHDF spreading on soft (ζ=0.7) silicone elastomers with immobilized fluorescent beads and coated with fibronectin. In this experiment, light exposure resulted in unintentional cell death. Beads accumulated under fibroblasts as a result of cell tractions in the initial stages of spreading, but did not recover their original positions following cell death. Scale bars: 20 μm. **D)** Confocal microscope images of pHDF seeded for 5 hours on soft (ζ=0.7) silicone elastomers with

immobilized fluorescent beads and coated with fibronectin (top). The cells were washed with PBS and treated with 0.5% trypsin-EDTA solution for 10 minutes (middle). Next, the medium over the cells was gently pipetted up and down to remove loosely attached cells (bottom). The fluorescent channel showed incomplete relaxation of the beads on the surface, which was not affected by cell removal over the substrate. The resolution and quality of the transmitted light images on the left was low, because they are constructed from the transmitted light during laser scanning of the area of interest. Nevertheless, rounded cells after trypsin treatment were identified (arrows), which were removed after pipetting. Scale bars: 20 μm.

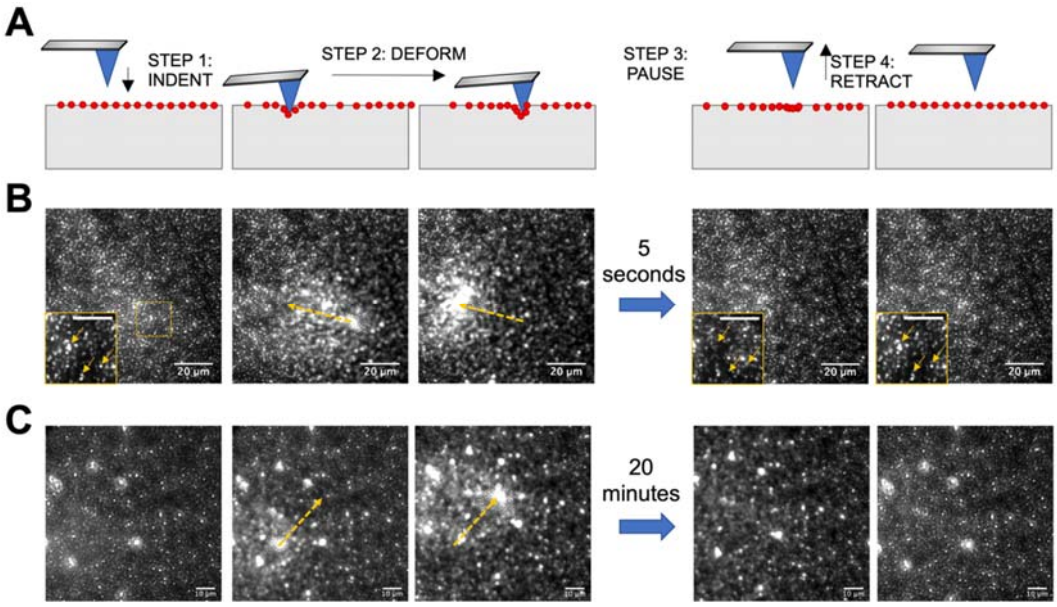


**Figure S7**. Elastomer surface does not display viscoplasticity after AFM tip-induced deformations. **A)** Schematic of the experimental setup used to indent the elastomer (step 1), laterally move the cantilever to induce deformation (step 2), optionally pause at the new position (step 3) and retract the cantilever (step 4). **B,C)** Still frames from time lapse imaging of the elastomer ($\zeta$=0.7) surface, on which fluorescent beads as fiducial markers have been immobilized and fibronectin was coated. Each frame corresponds to each step indicated in the schematic above. Dashed arrows indicate the lateral movement of the tip, which is not visible at the fluorescence channel. Insets in (**B**) show the boxed area and arrows are guides to the eye, to emphasize the movement of beads. After tip retraction, beads recover to their original position over a few minutes, despite large deformations applied. The pause in the deformed state was 5 seconds in (**B**) and 20 minutes in (**C**). Scale bars: (**B**) 20 µm, (**B inset**) 10 µm, (**C**) 10 µm.

## Supplementary Movie Legends

**Supplementary Movie 1.** Poking silicone elastomers with a metal spatula at 2x actual speed. The softer elastomer (ζ=0.7) is sticky and highly deformable, yet elastic, recovering back to its original position after loss of adhesion with the spatula. The stiffer elastomer (ζ=1.5) on the other hand, does not show considerable adhesion.

**Supplementary Movie 2.** Live-cell, time-lapse, fluorescence confocal microscopy of pHDF remodeling fluorescent fibronectin (FFN)-coated glass substrates. The first frame (t=0) was acquired 1hour after seeding.

**Supplementary Movie 3.** Live-cell, time-lapse epifluorescence microscopy of pHDF spreading on fluorescent fibronectin (FFN)-coated elastomers with ζ=0.7. The first frame (t=0) was acquired immediately after cell seeding.

**Supplementary Movie 4.** Live-cell, time-lapse epifluorescence microscopy of pHDF spreading on fluorescent fibronectin (FFN)-coated elastomers with ζ=1.0. The first frame (t=0) was acquired immediately after cell seeding.

**Supplementary Movie 5.** Live-cell, time-lapse epifluorescence microscopy of pHDF spreading on fluorescent fibronectin (FFN)-coated elastomers with ζ=1.5. The first frame (t=0) was acquired immediately after cell seeding.

**Supplementary Movie 6.** Live-cell, time-lapse fluorescence confocal microscopy of pHDF spreading on fluorescent fibronectin (FFN)-coated elastomers with ζ=0.7. The first frame (t=0) was acquired immediately after cell seeding. Scale bar: 20 μm.

**Supplementary Movie 7.** Live-cell, time-lapse epifluorescence microscopy of pHDF spreading on soft, fibronectin-coated elastomers (ζ=0.7) with immobilized fluorescent particles. The first frame (t=0) was acquired immediately after cell seeding. Fibroblasts rapidly accumulated the particles under their body.

**Supplementary Movie 8.** Live-cell, time-lapse fluorescence confocal microscopy of pHDF spreading on soft, fibronectin-coated elastomers (ζ=0.7) with immobilized fluorescent particles. The first frame (t=0) was acquired a few minutes after cell seeding. Scale bar: 20 μm.

**Supplementary Movie 9.** Live-cell, time-lapse fluorescence confocal microscopy of pHDF spreading on fibronectin-coated elastomers ($\zeta$=1.0) with immobilized fluorescent particles. The first frame (t=0) was acquired a few minutes after cell seeding. Scale bar: 20 μm.

**Supplementary Movie 10.** Live-cell, time-lapse fluorescence confocal microscopy of pHDF spreading on fibronectin-coated elastomers ($\zeta$=0.7) with immobilized fluorescent particles, along with the displacement fields calculated from the PIV analysis. The first frame (t=0) was acquired a few minutes after cell seeding. Scale bar: 20 μm.

**Supplementary Movie 11.** Live-cell, time-lapse fluorescence confocal microscopy of pHDF spreading on fibronectin-coated elastomers ($\zeta$=1.0) with immobilized fluorescent particles, along with the displacement fields calculated from the PIV analysis. The first frame (t=0) was acquired a few minutes after cell seeding. Scale bar: 20 μm.

**Supplementary Movie 12.** Time lapse imaging of fluorescent particles immobilized on the surface of a soft ($\zeta$=0.7) elastomer during AFM-induced deformations. A stiff cantilever with a conical tip was manually lowered on the surface of the elastomer and laterally moved to a new position to deform the substrate. After 5 seconds, the cantilever was retracted and the position of beads monitored over time. Scale bar: 20 μm.